sustainability

MDPI

Article

Sedimentation Pattern as a Response to Hydrodynamics in a Near-Symmetric River Confluence

João Nuno Fernandes [1,*] and Leila Alizadeh [2]

[1] National Laboratory for Civil Engineering, 1700-066 Lisbon, Portugal
[2] Civil Engineering Research and Innovation for Sustainability, Instituto Superior Técnico, Lisbon University, 1049-001 Lisbon, Portugal
* Correspondence: jnfernandes@lnec.pt

Abstract: River confluences are dynamic zones where hydrodynamic interactions between tributary flows—varying in velocity, direction, and sediment concentration—can significantly alter hydro morphology. These changes feature substantial consequences for the stability of riverbanks, nearby hydraulic structures, and the surrounding environment. This paper investigates flow mechanisms and sediment dynamics in a symmetric 50° confluence through laboratory experiments on a scaled physical model of a real confluence located on Madeira Island, Portugal. Acoustic Doppler velocity measurements were used to analyze the hydrodynamic characteristics, while bathymetry was surveyed using an RGB sensor and the Structure from Motion technique. Sedimentation patterns were correlated with key flow zones within the confluence. This study highlights how variations in discharge and momentum ratios influence sediment distribution and morphology, potentially destabilizing riverbanks and contributing to sediment deposition and erosion patterns. Understanding these mechanisms is critical for improving the sustainable management of water resources and minimizing anthropogenic impacts on fluvial systems. The findings provide valuable insights for enhancing river resilience, protecting natural watercourses, and supporting sustainable development by promoting informed planning of hydraulic structures and sediment management strategies.

Keywords: river confluences; tributaries; mixing layers; hydromorphology; flow structures

Academic Editors: Tommaso Caloiero and Hossein Bonakdari

Received: 12 February 2025
Revised: 4 April 2025
Accepted: 11 April 2025
Published: 23 April 2025

Citation: Fernandes, J.N.; Alizadeh, L. Sedimentation Pattern as a Response to Hydrodynamics in a Near-Symmetric River Confluence. *Sustainability* **2025**, *17*, 3790. https://doi.org/10.3390/su17093790

1. Introduction

The interaction of two streams at fluvial confluences leads to significant transfers of mass and momentum, establishing these nodes as critical elements of the fluvial corridor. The interactions can profoundly influence downstream conditions by introducing water, sediment, wood, or ice into the main river system (cf. [1]). Differences in velocity, flow direction, and sediment concentration between tributaries create complex hydrodynamic and morphodynamic processes in the downstream reach. Due to the inherent complexity of these processes, scientific investigations into river channel confluences have evolved gradually over time [2].

The flow mechanisms in fluvial confluences are primarily governed by the mixing of tributary flows. Mosley [3] distinguished between symmetrical confluences, where tributaries merge to form a new downstream channel, and asymmetrical confluence, where a tributary joins a main channel laterally. In symmetrical confluences, the main flow mechanisms, as illustrated in Figure 1, include flow stagnation immediately downstream of the junction, deflection of the tributary flow, flow separation zones, shear layers, maximum velocity regions, gradual flow recovery, and secondary currents (see, for example, [3,4]).

These mechanisms play a critical role in determining the spatial and temporal distribution of flow velocities and sediment transport, influencing the long-term morphology and stability of the confluence zone.

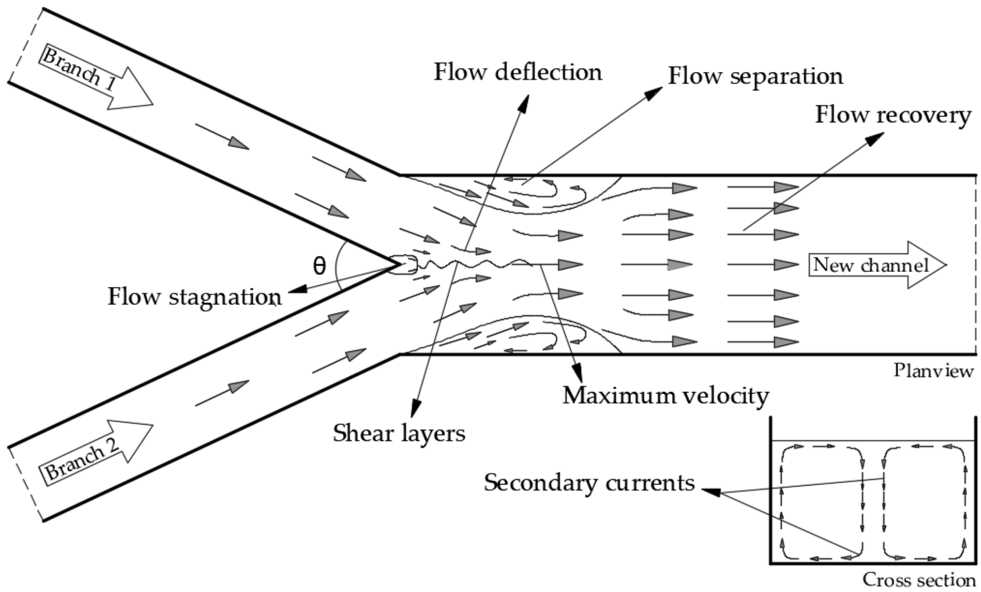

Figure 1. Main flow mechanisms in symmetrical confluences (adapted from [5]).

The geometry of a confluence significantly influences flow structures, with factors such as confluence angle (θ), momentum and discharge ratios, and symmetry playing key roles [5]. Increased confluence angles have been linked to enhanced flow stagnation and separation [6]. While most flow studies use in situ or laboratory methods, Bradbrook et al. [7] employed numerical approaches to show the effects of confluence angles and tributary turbulence on downstream flow. Similarly, Nazari-Sharabian et al. [8] developed numerical guidelines for managing flooding at a submerged drainage confluence. Confluences with bed discordance distort mixing layers as deeper channel flows laterally entrain into the separation zones [9]. Downstream of such confluences, secondary cells form between jet flows and inner banks.

Understanding the influence of flow dynamics on sedimentation is essential for effective river management, as erosion affects riverbank stability, vegetation, and sediment deposition [10]. While clear water flow mechanisms are well-studied, sediment transport processes at confluences remain less explored [11]. Guillén-Ludeña et al. [12,13] studied hydro-morphological processes in confluences where narrow, steep tributaries join wide, low-gradient main channels. They observed key discordant features, such as a so-called avalanche face at the tributary mouth and a bank-attached bar in the post-confluence zone, highlighting areas of significant sediment deposition and erosion. In mountain river confluences, junction angle and discharge ratio were identified as critical factors influencing hydrodynamics and morphology. High sediment loads from tributaries contribute to bed discordance, affecting flow, habitat, flood risk, and sediment management.

For steep tributaries with high sediment loads, Leite Ribeiro et al. [14] identified significant bed discordance due to contrasting flow regimes: tributary flows occupy upper layers, while the main channel dominates the lower layers, shaping downstream sedimentation patterns.

The impact of shear layer distortion on turbulent flow structures in asymmetric channel confluences was demonstrated by Yuan et al. [15], who found stronger helical cells formed when tributary flow rates exceeded those of the main channel. Key turbulence characteristics—such as Reynolds shear stress, maximum turbulent kinetic energy, and ejection and sweep events—were concentrated at mid-water depths, closely tied to shear layer distortion. Higher discharge ratios increased velocity, turbulence, and shear stress, while reduced discharge amplified shear layer distortion. These insights are essential for understanding sediment transport, as turbulent structures and shear stresses drive sediment entrainment, transport, and deposition.

The influence of sediment discharge on the morphology of a movable bed in an asymmetric open channel confluence was investigated by Bombar and Cardoso [16]. The authors observed that larger sediment inputs, associated with higher stream powers, caused significant morphological changes for a given water discharge ratio. Similarly, Lewis and Rhoads [17] measured real-world hydrodynamics, linking flow mechanisms to scour hole formation. Higher discharges produced pronounced scour near the margins, while lower discharges shifted scour holes toward the channel center. Helical currents and shear layers emerged as key influencing factors.

A defining feature of confluence flow mechanisms is shear layer distortion, caused by tributary flow penetrating the main channel [15]. This behavior distinguishes confluences from other sheared flows, such as compound channels (e.g., [18]). Zhang et al. [19] explored hydrodynamics and bed morphology at the confluence of the sediment-laden Yellow River and the clear Fen River, revealing elevated water surfaces in stagnation zones and lower elevations at the junction corner. The size and location of critical regions—such as stagnation zones, acceleration areas, shear layers, and flow recovery zones—were primarily shaped by momentum transfer ratios.

Nazari-Giglou et al. [20] examined the flow and geometrical conditions leading to sediment motion in channel confluences, emphasizing the significance of flow velocity, confluence angle, discharge and width ratios, and bed material properties. These factors play a vital role in predicting sediment transport and deposition patterns, which are fundamental for river engineering, habitat restoration, and sediment management practices.

This highlights the importance of sediment transport studies in confluences, as variations in sediment load and flow conditions can lead to substantial changes in channel morphology, affecting floodplain stability and infrastructure. Understanding these patterns is crucial, as the formation and evolution of scour holes can influence sediment routing, habitat structures, and the long-term stability of confluence zones.

This paper investigates the three-dimensional flow structure and turbulence field in a symmetric 50° confluence, aiming to establish links between these hydrodynamic features and observed riverbed hydromorphology. A non-distorted 1:60 scale physical model of the confluence was developed for experimental purposes. Following Alizadeh and Fernandes [21], controlled experiments were conducted to analyze the effects of tributary momentum and width ratios on hydrodynamics and sediment routing. Velocity fields for five flow cases with varying tributary momentum and width ratios were measured using acoustic Doppler velocimetry. These high-frequency measurements allowed the characterization of the turbulent statistics. Additionally, sedimentation patterns downstream of the confluence were characterized through point measurements, infrared imaging, and photogrammetry. These findings are critical for managing sediment transport in natural and engineered river systems, supporting aquatic habitat stability, and improving sediment management strategies.

The scientific gaps addressed in this study primarily relate to the limited understanding of sediment transport dynamics and hydrodynamic interactions in symmetric river confluences. While previous research has extensively investigated flow structures and turbulence in natural and experimental settings, sediment transport mechanisms remain insufficiently explored, particularly in controlled laboratory environments. Many studies have focused on clear-water hydrodynamics, often neglecting the complex interplay between flow structures, sediment entrainment, and deposition. Additionally, existing research has predominantly examined asymmetric confluences, leaving a gap in knowledge regarding sedimentation patterns in (near-)symmetric confluences, where tributary momentum and discharge ratios play a crucial role in shaping riverbed morphology. The absence of high-resolution experimental studies has further constrained the development of analytical models for sediment transport in engineered and natural river systems.

Using acoustic Doppler velocimetry, photogrammetry, and RGB sensor-based bathymetric surveys, this study provides high-resolution data on sedimentation patterns and hydrodynamic interactions. The findings reveal the impact of tributary momentum and discharge ratios on sediment deposition, scour formation, and shear layer development. These insights enhance the understanding of sediment transport processes in confluences, offering valuable guidance for sustainable river management, flood risk mitigation, and hydraulic structures management. This study also contributes to refining numerical models by providing empirical data that can improve the accuracy of sediment transport simulations in river confluences.

2. Materials and Methods

2.1. Site and Scaled Model

The experiments were conducted in a model of a symmetric confluence located in Funchal, Madeira Island, Portugal. João Gomes and Santa Luzia Creeks are the two tributaries that join in a confluence at coordinates 32°38′49.7′′ N and 16°54′17.9′′ W and flow directly to the Atlantic Ocean, as presented in Figure 2a,c.

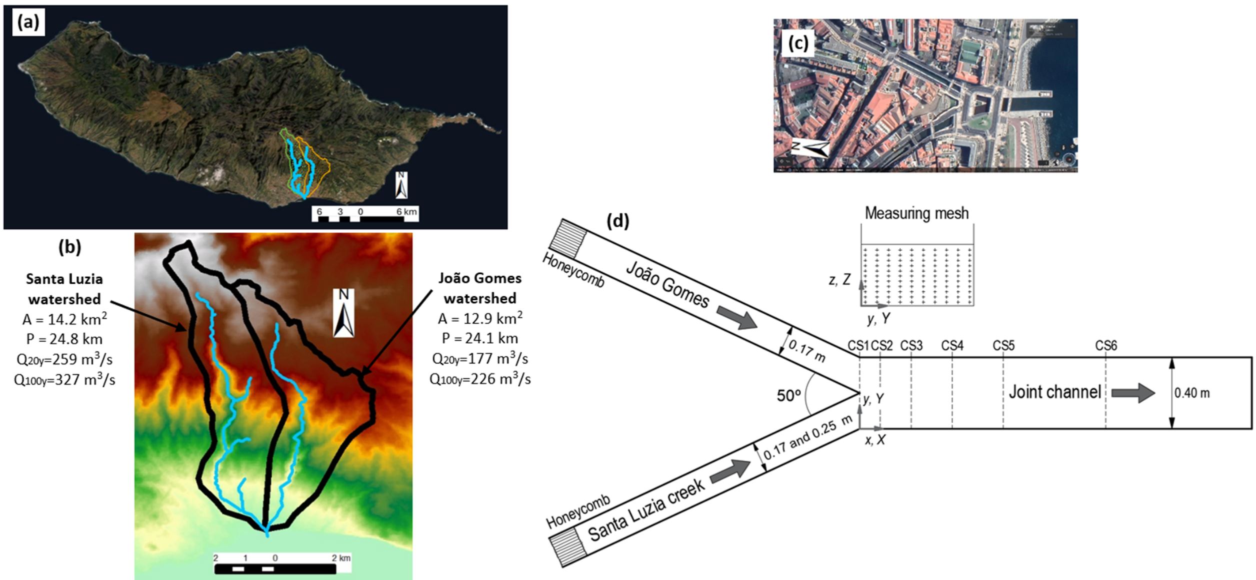

Figure 2. (**a**) Location of the watersheds on Madeira Island; (**b**) hipsometry and watershed characteristics; (**c**) Google aerial view; (**d**) schematic representation of the confluence flume.

The watersheds of these creeks are presented in the hypsometric map in Figure 2b. They have a similar area and shape, and as the soil characteristics are also approximately the same, previous studies showed that the sediment transport due to a 100-year return period flood are similar for both tributaries. Figure 2b also features the corresponding flood discharge flows for return periods of 20 and 100 years. The land use is predominantly forest and urbanization. The final reach comprises a confluence that was constructed in concrete as a regularized channel.

In order to study the hydrodynamic characteristics and sediment transport in this confluence, a 1:60 scale model was constructed at the National Laboratory for Civil Engineering (LNEC) in Lisbon, Portugal. For this open-channel model, Froude similarity was used due to the highly turbulent phenomena and the fact that energy dissipation depends mainly on turbulent shear stress terms [22].

In the flume, João Gomes and Santa Luzia creeks were designated as tributaries 1 and 2, respectively, with widths (b1 and b2) of 0.17 m and 0.25 m and heights of 0.25 m each. The joint channel is a concrete structure with a width (b3) of 0.40 m and a height of 0.15 m. Additional experiments were conducted by reducing the width of Tributary 2 to 0.17 m to analyze its influence during the experimental campaign, achieving a fully symmetrical configuration in this case. Both tributaries have a slope of 0.028 m/m, while the joint channel is horizontal. A schematic representation of the experimental recirculating hydraulic circuit is shown in Figure 2d.

The streamwise flow alignment was provided by a 3 cm diameter and 30 cm long circular honeycomb screen located upstream in each tributary. This screen improved the approach flow and the transition between the constant level reservoirs (not represented) and the tributary channels. In the downstream section, a flap tailgate imposes the subcritical flow depth.

2.2. Control Variables and Parameters

This experimental study aimed to characterize how channel width and momentum ratio influence flow structure and sediment transport in confluences. To achieve this goal, five flow cases, labeled FC1 to FC5, were conducted. Table 1 summarizes the key parameters of these experiments. Each flow case features a constant discharge in each tributary, denoted as Q_1 and Q_2. Additionally, the corresponding momentum transfer, calculated as $M = \rho\, QU$ (where ρ is the volumetric mass density and U is the cross-sectional averaged velocity), is provided.

Table 1. Characteristics of the flow cases (FCs).

Flow Case	b_1 (m)	$b_{2.5}$ (m)	Q_1 (l s^{-1})	Q_2 (l s^{-1})	Q_2/Q_1	M_1 (kg m s^{-2})	M_2 (kg m s^{-2})	M_1/M_2	Fr_1	Fr_2	Re_1 ($\times 10^4$)	Re_2 ($\times 10^4$)	Sediment Discharge (l/s)	
													1	2
FC1	0.17	0.25	7	3	0.4	2.86	0.33	8.6	0.60	0.14	7.94	2.69	0.007	0.011
FC2	0.17	0.25	3	7	2.3	0.49	1.79	0.23	0.24	0.34	3.29	6.29	0.007	0.011
FC3	0.17	0.25	5	5	1	1.35	0.90	1.5	0.39	0.23	5.44	4.46	0.007	0.011
FC4	0.17	0.17	5	5	1	1.32	1.34	0.98	0.38	0.39	5.36	5.41	0.007	0.011
FC5	0.17	0.17	3	7	2.3	0.48	2.62	0.18	0.23	0.54	3.22	7.56	0.007	0.011

The table also includes the Froude number ($Fr = U/\sqrt{gh}$, where g is the acceleration due to gravity and h is the flow depth) and the Reynolds number ($Re = 4UR/\nu$, where R is the hydraulic radius and ν is the kinematic viscosity). These parameters are crucial for understanding the dynamics of flow in the experimental setup and provide insights into the hydraulic conditions governing sediment transport and flow characteristics at the confluence.

Figure 2d shows the Cartesian orthogonal coordinate system (the x, y, z and u, v, w symbols were used for position and velocities in longitudinal, transverse, and vertical directions, respectively). The origin is located on the right side, downstream of the confluence. When relevant, the positions x, y, and z were nondimensionalized by the downstream channel width, B_m. These normalized variables were named X = x/B_m, Y = y/B_m, and Z = z/B_m. As only one flow case features complete "symmetric" conditions, this confluence may be referred as "nearly-symmetric".

The sedimentation was characterized in additional experiments for the five flow cases. The sediment load was fixed according to the 100 years return period flood for tributaries 1 and 2, respectively. These sediments were steadily placed in the upstream section of each tributary during 1 h (according to Froude similarity). At the beginning of the experiment, the joint channel downstream of the tributaries was empty and without any sediment. This setup was designed to simulate actual conditions observed on Madeira Island.

Using a similar Shields parameter, these sediments were characterized by a mean diameter d_{50} = 0.43 mm (corresponding to 3.2 mm in the prototype) and a bulk mass density of 1250 kg/m^3.

2.3. Equipment and Measuring Meshes

The discharge of each tributary was measured by two dedicated electromagnetic flowmeters with a precision equal to 0.01 l/s.

Water depths were measured as the difference between the water surface and bottom elevations, as given by an ultrasonic probe (UNDK 20I6903/S35A from Baumer, Frauenfeld, Switzerland).

A Vectrino Accoustic Doppler Velocimeter from Nortek, Sandvika, Norway (with an acquisition frequency of 100 Hz) was used to measure the 3 velocity components. The measurement uncertainty in velocity is $\pm$0.5% of the measured value or $\pm$1 mm.s^{-1}.

Measurement cross sections (CS1 to CS6) are presented in Figure 2d. Each one of these 6 cross sections comprised a total of 80 measuring points (10 equidistant verticals of 8 points each).

Following the procedures and the setup defined in Goring and Nikora [23] and Fernande and Jónatas [24], in each point, 9000 samples (90 s times 100 samples per second) were collected, and the phase-space threshold despiking method was used to treat and filter the raw velocity data.

Two main techniques were used to characterize the sedimentation pattern. After the experiment, during the equilibrium phase, the flume was drained very slowly to preserve the final sedimentation pattern. Using this preserved bottom, a 3D reconstruction was performed with Structure from Motion (SfM) and an RGB sensor to obtain a detailed point cloud of the bathymetry.

The application VisualSFM proposed by Wu [25] was used for the 3D reconstruction using the SfM technique. This photogrammetric method is based on a set of multiple photographs collected from different angles.

An RGB sensor (MS Kinect from Microsoft, Seatle, WA, USA) was used to automatically obtain this point cloud. This sensor comprised a color camera and a depth sensor. The resolutions of the RGB and depth images were 1920 $\times$ 1080 px and 640 $\times$ 480 px, respectively. The frame rate was 30 fps, and the measurement distance range of the target objects in this study was between 170 and 320 cm. Point cloud data were treated using the Cloud Compare v.2.13 software.

At the end, additional point gauge measurements were collected to calibrate and validate the results obtained from the previous techniques.

3. Flow Mechanisms

As the geometric characteristics of the joint channel and total discharge remain constant during the experiments, the water surface profile was mainly determined by the position of the downstream tailgate. Previous results published in Alizadeh and Fernandes [21] revealed that the water surface profile was approximately the same for all flow cases.

Figure 3 presents the non-dimensional streamwise velocity magnitude u/U, where u is the streamwise velocity and U is the mean cross sectional streamwise velocity. These results are presented for the 6 cross sections identified in Figure 2d, ranging from CS1 in the top row to CS6 in the lower row, and for the 5 flow cases, from FC1 in the first column to FC5 in the last column. In the same plots, the vectors corresponding to the secondary flows (v for spanwise and w for vertical velocities) are also presented.

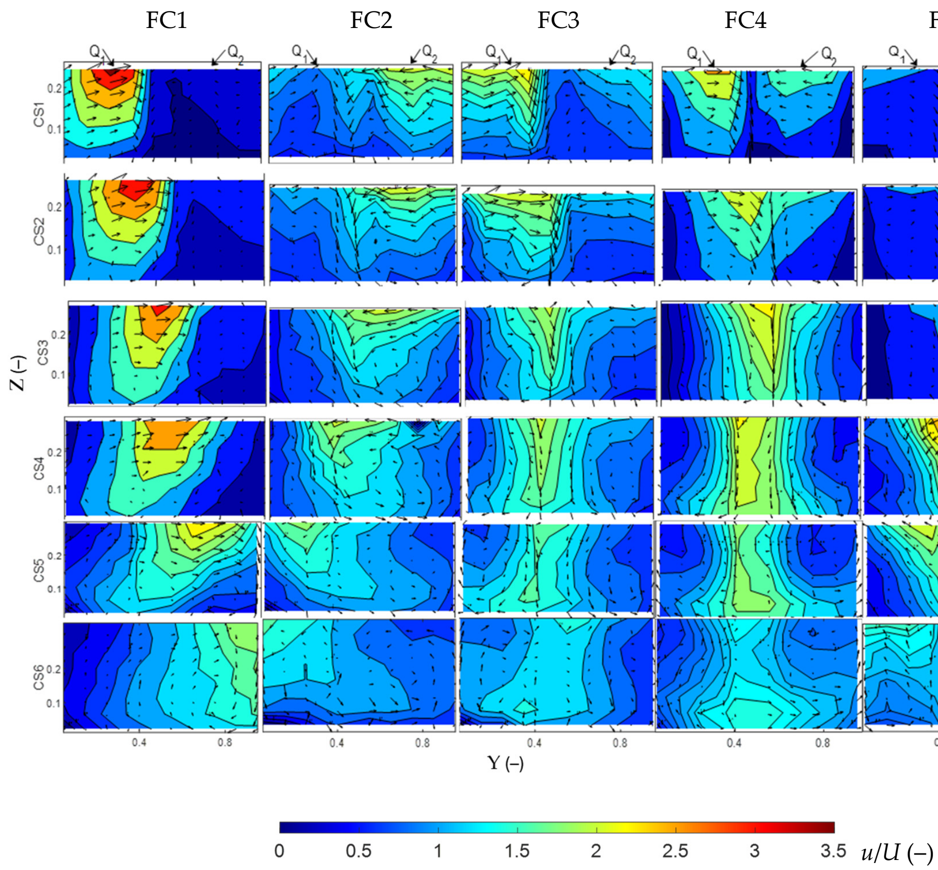

Figure 3. Non-dimensional streamwise velocity magnitude u/U and secondary flow vectors (columns correspond to the 5 flow cases and rows stand for the 6 cross sections).

The secondary flows plotted in Figure 3 reveal that strong secondary currents are observed at the beginning of the joint channel (e.g., the first measurement cross section) for all flow cases. These currents are mainly driven by the momentum ratio. For FC1, only one secondary flow is observed, whereas FC2 to FC5 feature two secondary cells with opposite direction (one for each tributary flow). For these latter flow cases, the two secondary currents seem to be maintained until the last cross section. For FC1, it is observed that the flow velocity of tributary 1 enhances the magnitude of this secondary cell, which becomes dominant in the last cross sections.

Corroborating the conclusion from [4], velocity differences from the near bed to the surface are rather high, making depth average models (i.e., 2D modelling) not suitable for the complete description of the mixing processes. Even with the same junction angle, very different secondary patterns were obtained, which is in accordance to the findings of Bradrook et al. [7], who consider the velocity and momentum ratio as key factors influencing secondary currents.

Comparing FC1 and FC2 (same discharge distribution but different width), when lower discharge comes from a wider tributary (as in FC5), the jet flow is not so pronounced.

The distribution of the non-dimensional velocity magnitude $UV = \sqrt{(u/U)^2 + (v/U)^2}$ and the spanwise and streamwise velocity vectors u and v are presented in Figure 4a. To provide a clear presentation, only one of the 8 positions of the plan views for five flow cases are displayed at Z = 8.

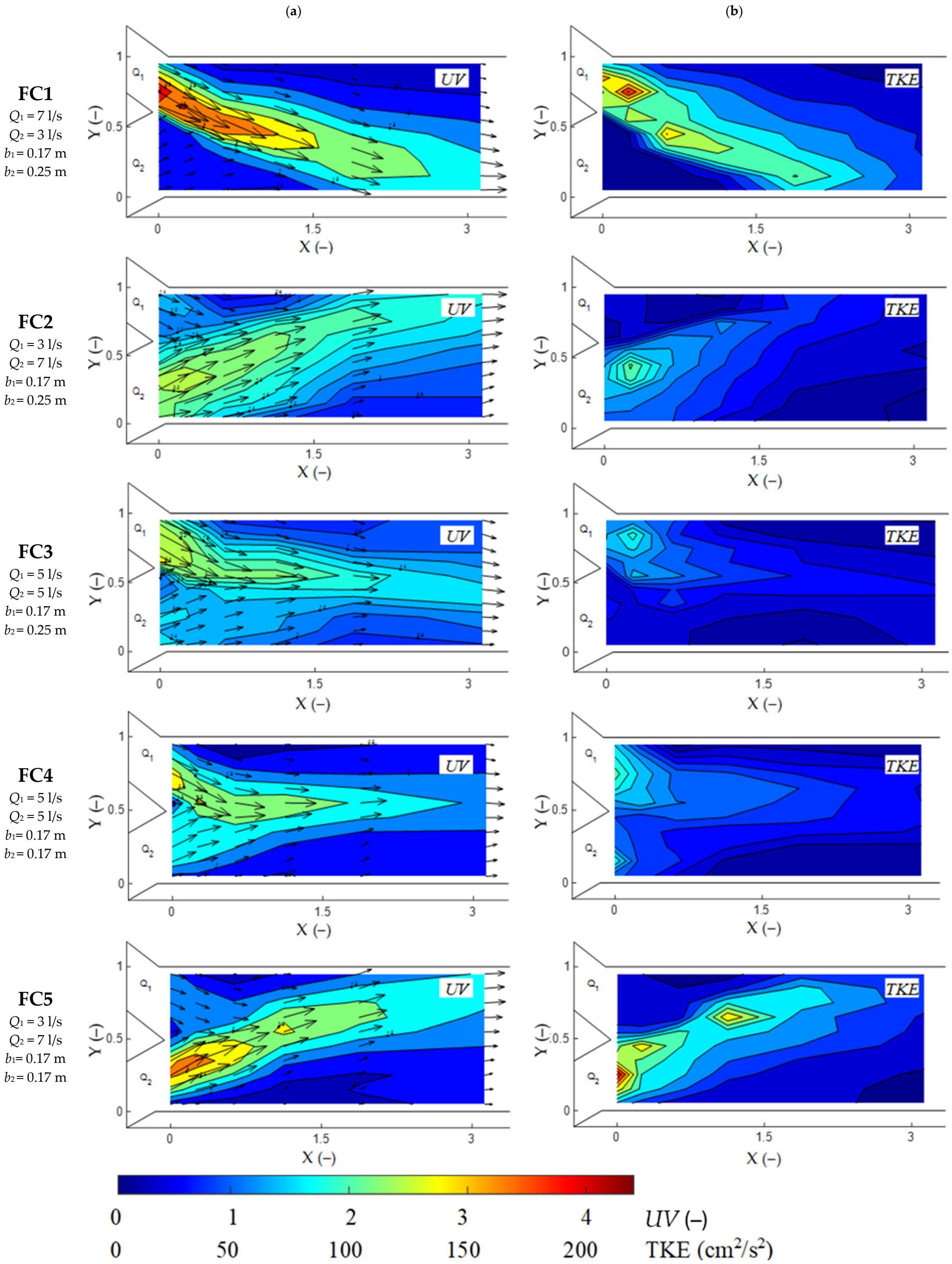

Figure 4. (**a**) Non-dimensional velocity magnitude UV and spanwise and streamwise velocity vectors u and v (in the left column) and (**b**) turbulent kinetic energy (in the left column).

The region of flow recovery is observed more downstream when the discharge ratio is far from 1. For flow cases 3 and 4, featuring Q_2/Q_1 = 1, despite some influence of spanwise flow, flow recovery is faster and transverse symmetry is achieved at the end of the flume.

Due to the abrupt change in the boundary geometry, tributary flows do not remain connected to the joint channel margins and flow separation is detected. This region is observed near the side walls for all flow cases along whole flow depth. Momentum ratio plays an important role in this flow element as it seems to influence its streamwise development. This is particularly evident for FC1 and FC5 that feature momentum ratios far from 1. Inverse flow in the flow separation region is not observed due to the relatively low angle between tributaries. As expected, boundary shear stress leads to the reduction of velocities near the bottom.

The interaction of the tributary flows at the confluence is one cause for the formation of the stagnation zone due to flow obstruction. This zone is obvious for FC4 near the surface, with both momentum and width ratio equal to one. Downstream to this stagnation region flow deflection is observed in joint channel. This region is visible over the whole junction depth but more evident and wider near the channel bed. Results seem to confirm Riley & Rhoads [6] observation that flow deflection is mainly controlled by the momentum ratio between the tributaries.

Regarding turbulence characteristics, for the same conditions as presented in Table 1, ref. [22] showed the cross-sectional distribution of turbulent kinetic energy ($TKE = 0.5\left(\overline{u'u'} + \overline{v'v'} + \overline{w'w'}\right)$, where u', v', and w' stand for the fluctuating velocity components by Reynolds decomposition. Figure 4b presents the plan view of TKE for the vertical position Z = 8.

It was observed that TKE gradually decreased towards the channel wall and towards the bed. The maximum values of TKE occurred close to the joint of the tributaries (at approximately 10 cm). For flow cases with high momentum ratios (FC5 and FC1), there was a strong jet flow that hit the wall at cross-section 6, causing high gradients of momentum and velocity. The results are rather similar for FC3 and FC4 (FCs that feature momentum ratios close to 1). In these cases, a low magnitude of turbulent kinetic energy was observed.

In all FCs, as flow progresses in the joint channel, turbulence kinetic energy decreases, and at the end of the joint channel, a more stable flow is observed (flow recovery).

4. Morphodynamics

Sediments were steadily added at the upstream section (near the honeycombs in Figure 2d), flowing through each tributary toward the confluence. Sediment feeding lasted 1 h, simulating an 8 h real-world event based on Froude similarity. The simulation was derived from a 100-year return period and was applied equally to both tributaries. The sediments were eroded, transported, and deposited according to stream power and boundary shear stress. During the feeding period, the sedimentation pattern evolved and was monitored primarily through observation and photographs, as bathymetry measurements were not possible. It was clear that the equilibrium was not reached by the end of the feeding period, so experiments continued for approximately 6 more hours, until a constant sedimentation pattern indicated equilibrium. Control points were monitored to determine when this phase was achieved.

The final sedimentation configuration in the equilibrium phase was assessed using 3D reconstruction with photogrammetry and a kinetic sensor, with manual point gauge checks for control and monitoring. These river morphological patterns in confluences have significant implications for the management and design of river channels. Confluences are often sites for flooding, ice jams, and bed and bank instability, which are critical concerns, as they can threaten riverine infrastructure such as buildings and river docks.

Nazari-Giglou et al. [20] emphasize the importance of predicting scour depth for the design of bridges near confluences. Buildings and other structures located near riverbanks can also be affected by these morphodynamic processes.

Figure 5 illustrates the bed morphology for the five flow cases identified in Table 1. In the figure, the scale refers to the sediment layer in the channel.

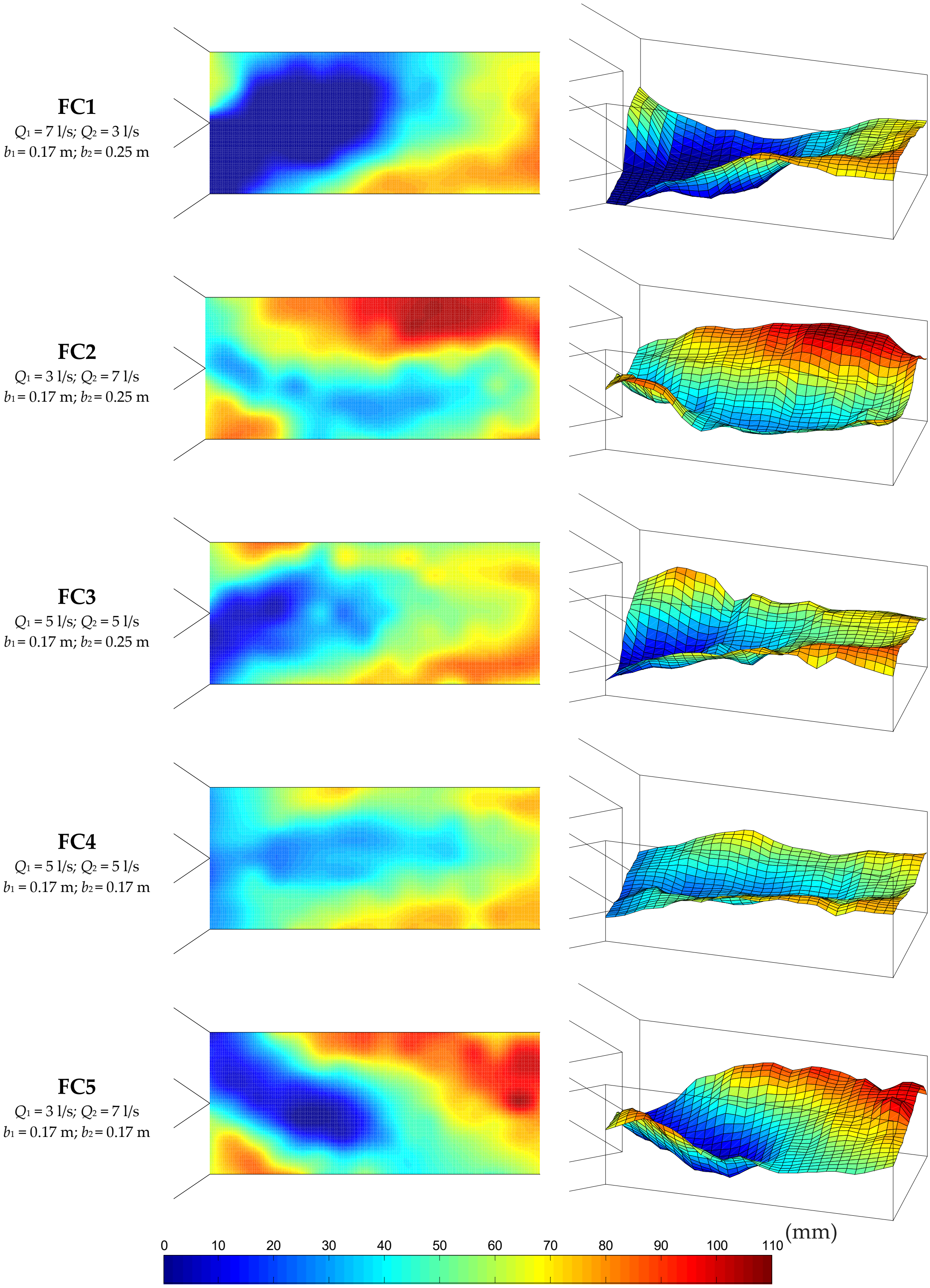

Figure 5. Bed morphology for five flow cases in equilibrium.

Understanding sediment transport and morphodynamic patterns in river confluences is essential for mitigating risks associated with flooding and structural instability. Effective management and design strategies rely on accurate predictions of these processes to protect infrastructure and ensure the safety and functionality of river channels.

Figure 6 shows the cumulative sediment volume along the longitudinal direction of the joint channel.

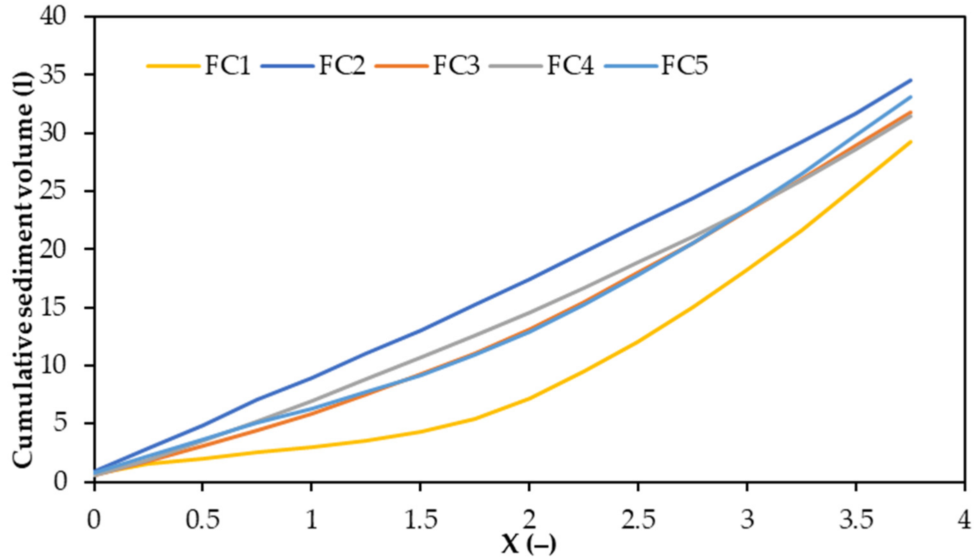

Figure 6. Cumulative sediment volume along the channel.

When in equilibrium, the typical morphological pattern in symmetric river confluences includes the following main characteristics:

(a) A bed transition between each tributary and the joint channel (this discordance can be so marked that it may be named avalanche slope);
(b) A deep local scour located right downstream of the confluence or aligned with the tributary direction;
(c) A dune or bar located in the middle of the joint channel;
(d) A dune or bar located in the lateral region of the joint channel downstream of the scour in the separation area;
(e) Sediment accumulation near the junction (in the flow stagnation area).

Despite the different patterns for each flow case, some of these elements can be globally identified in the morphological profile observed.

Figure 6 shows that, except for FC1, despite the different cross-sectional distributions along the channel, the results for the accumulated settled volume are generally comparable along the channel. These configurations, which involve different inlet configurations, promote similar sediment transport, and sediment is more evenly distributed along the channel length.

The typical features regarding the morphodynamics in sand- and gravel-bed confluences are a central scour hole, tributary mouth bars, and bank-attached bars in areas of flow recirculation and stagnation. The physical factors influencing confluence hydraulics and the resulting morphology include junction angle, bed discordance, discharge ratio, and upstream planform curvature.

The general pattern comprises a scour corridor aligned with the tributary with the highest momentum and velocity. This aspect is particularly evident for flow cases FC1 and FC5, which feature a high momentum ratio between the tributary flows. For the first flow case, it is observed that a very strong scour hole aligned with tributary 1 (highest discharge and lowest width). This configuration of the tributary leads to very high average velocity that seems to increase the stream power to lift, transport, and divert sediments towards downstream. This increase of the scour corridor from tributary 1 is complemented by a mouth bar in the alignment of tributary 2. The same pattern is also observed in FC5 and, to a lesser extent, in FC3 and FC2. However, in these two latter FCs, a pronounced bank-attached bar is observed near the wall of the lower average velocity.

The morphological configuration obtained in the equilibrium phase for the experiments with high discharge ratios seems to be characterized by strong scour leading to a excavated hole from one tributary and much less scour in the alignment of the second tributary. This process leads to an "avalanche" profile in this first tributary and it corresponds to the typical bed discordance confluences with uneven bed elevation and relatively steep slopes, identified in many cases with the beginning of systematic bathymetric surveys (e.g., [9]).

Together with the influence of the secondary currents, the shear layer formed in the interface of the tributary flows plays an important role in the increase of boundary shear stress and of the scouring process. From our experiments, it is important to point out that secondary currents were present with the channel even in the absence of sediments.

Characterized by symmetric geometry and equal discharge and momentum between the tributaries, FC4 is also characterized by a rather symmetric morphologic pattern. In this flow case, together with the central scour hole, banks are formed near the lateral walls. It is interesting to compare the formation of these side banks and their longitudinal evolution with the secondary current vectors (cf. Figure 3). Together with the increasing velocity magnitude, which leads to an increase in boundary shear stress, the downward flow in the center of the joint channel helps to lift sediments. Spanwise velocities transfer these sediments from the center towards the lateral banks which eventually deposit in the lateral bars. This mechanism can be observed in all flow cases, but in FC4, it is particularly evident, as there are no other spanwise differences or any other triggering factors influencing the morphological pattern. The influence of secondary currents seems to be crucial for this pattern.

Besides this feature, an additional interesting pattern is also clear in FC4. After the first central scour hole, a second one is formed downstream. Even though it is less evident, the same pattern also occurs for FC2 and FC3. This feature may be due to the deposit of the sediments diverted from the first main scour hole. With the decrease in velocity observed in Figure 4, these sediments form a small central bar. The eroded material that came from the scour hole was directly deposited downstream uniformly with respect to the alignment of the scour corridor.

The importance of the secondary currents for the formation of the lateral bars is also marked when one tries to link the direction and magnitude of these currents and the sedimentation near the banks. The strong secondary currents of FC2 and FC5 lead to the formation of high sedimentation in these cases, for instance. Following a numerical modelling approach, Bradbrook et al. [7] revealed the occurrence of secondary currents even without any topographic forcing. In the present work, it seems clear that these currents are a consequence of the mixture between the tributary flows and that they enhance the scour hole. With the increase in scouring, the secondary currents are also enhanced.

Discordant bed confluences are due to different conditions of sediment transport upstream. In this case, despite a concordant bed at the beginning of the experiments, very different bed elevations were obtained, depending on the flow and momentum ratios. Boyer et al. [26] studied the flow structure in a discordance confluence and investigated the effects on sediment transport by measuring near-bed flow turbulence, bed load transport rates, and changes in bed morphology for different flow conditions. High sediment transport rates are found at the edges of the shear layer region where the horizontal-vertical cross stresses are high. These features correspond to changes in bed morphology where erosion takes place along the shear layer. In our case, it seems that this pattern is followed, as high scour occurred typically in high shear regions (identified by high TKE in Figure 4). This feature highlights the importance of the shear layer for the sediment transport, as already suggested by Yuan et al. [15].

Flow hydrodynamics in a confluence plays a critical role in determining sediment scouring and deposition patterns. The distribution of flow across the cross sections, coupled with the influence of secondary flows, creates zones of high and low shear stresses that govern sediment behavior. For instance, areas with strong secondary currents, influenced by the tributary momentum ratio and flow deflection, enhance sediment scouring by increasing turbulence and boundary shear stress. Conversely, zones of flow stagnation or reduced velocity, such as those observed near the interface of tributaries or in downstream flow recovery regions, promote sediment deposition.

The shear layer contributes significantly to sediment redistribution. Its distortion, caused by the interaction between tributary flows, creates high-turbulence regions that drive sediment entrainment and transport. The interplay of these flow mechanisms supports the development of key morphological features, such as scour holes, sediment bars, and bed discordance, as highlighted in the experiments. In cases with higher tributary momentum, sediment scouring is more pronounced along the flow-aligned scour corridor, with eroded material being transported downstream before settling in lower-energy regions. In contrast, for more balanced discharge ratios, sediment distribution is more uniform, with deposition occurring in predictable patterns, such as mid-channel dunes and lateral bars. These findings align with previous studies on sediment transport in river confluences, reinforcing the importance of tributary flow conditions in determining confluence morphology. The formation of avalanche slopes and bed discordance in certain flow cases further supports the role of momentum asymmetry in shaping sedimentation patterns.

The findings align with previous studies, such as those by Yuan et al. [15] and Bombar and Cardoso [16], which emphasize the role of turbulence in sediment transport dynamics. Similar to these studies, the observed scouring and deposition patterns in the scale model reflect the influence of momentum and width ratios on hydromorphological processes. However, notable differences emerge, such as the specific length and depth of scour corridors, which may be attributed to variations in experimental setup, sediment characteristics, or confluence angles.

5. Discussion

5.1. Hydrodynamic Interactions and Flow Recovery

The results reveal an important influence of tributary momentum and discharge ratios on flow structures at the confluence. Velocity measurements demonstrated that stronger secondary currents developed when momentum ratios were high, with counter-rotating cells persisting downstream. In flow cases with balanced discharge ratios (such as FC3 and FC4), flow recovery occurred faster, leading to more uniform velocity distributions. In contrast, flow cases with significant momentum asymmetry (e.g., FC1 and FC5) exhibited prolonged turbulence, delaying flow recovery and intensifying sediment scouring.

The formation of flow separation zones and stagnation areas aligns with findings from past studies, confirming that momentum transfer between tributaries governs shear layer dynamics. Notably, for cases with extreme momentum asymmetry, jet flows persisted longer, deflecting towards the channel walls and driving turbulent kinetic energy peaks. This extended turbulence intensified sediment transport, contributing to scour formation and sediment redistribution.

5.2. Sedimentation Patterns and Morphodynamic Features

The sedimentation experiments revealed distinctive morphological features that evolved based on flow conditions. The key features observed included:

- Central Scour Hole and Avalanche Slopes: High-momentum tributaries (as in FC1 and FC5) produced deep scour holes aligned with the dominant flow, with sediments diverted downstream. This pattern is consistent with real-world observations in mountain river confluences, where steep slopes and high stream power enhance sediment entrainment.
- Mouth and Bank-Attached Bars: Flow separation zones promoted sediment deposition, forming bars near the channel walls. These lateral features were more pronounced in flow cases with secondary currents of greater magnitude (e.g., FC2 and FC5), reinforcing the role of spanwise velocity components in sediment transport.
- Secondary Scour Holes: In symmetric flow conditions (FC4), a secondary scour hole formed downstream, likely due to sediment deposition from the initial scour zone. This finding highlights the cyclical nature of sediment transport, where flow deceleration downstream of high-energy zones promotes sediment settling and localized scour resurgence.

The results corroborate previous research, emphasizing the link between turbulence intensity and sediment dynamics. The shear layer distortion—exacerbated by momentum asymmetry—created high-energy zones that promoted sediment entrainment, while low-velocity regions acted as sediment sinks.

5.3. Practical Implications for River Management

These findings are critical for sustainable river management. Understanding the hydrodynamic forces driving sediment transport can inform strategies to mitigate erosion and infrastructure damage. For instance:

- Flood risk management: insights into scour hole formation can guide the placement of scour protection structures, reducing the risk of channel instability and bank collapse during extreme flood events.
- Sediment management strategies: predicting sediment deposition zones can help optimize dredging schedules, reducing maintenance costs and preventing channel blockages that could exacerbate flooding.
- Ecosystem restoration: Low-velocity regions downstream of the confluence may serve as natural habitats for aquatic species. Targeted habitat restoration efforts could enhance sediment retention and promote biodiversity, contributing to the overall resilience of river ecosystems.

5.4. Future Research

The high-resolution experimental data generated in this study provide a valuable benchmark for validating numerical models of sediment transport in river confluences. The detailed velocity fields, turbulence characteristics, and sedimentation patterns offer empirical evidence to refine model parameters, improving the predictive accuracy of hydro morphological simulations.

Future research could explore long-term morphological evolution under varying sediment loads and flow regimes, extending the experimental findings to more complex real-world scenarios. Additionally, the effect of the rigid boundaries and the influence of vegetation on sediment dynamics could offer new insights into nature-based solutions for flood mitigation and riverbank stabilization.

6. Conclusions

At river confluences, tributary flows interact to form a complex hydrodynamic interface, influenced by velocity, momentum, and direction differences. These interactions shape sedimentation patterns, impacting river structures and bank stability. This study used a 1:60 scale physical model of a 50° confluence on Madeira Island to analyze sedimentation patterns under 20- and 100-year flood scenarios. Five flow cases with varying flow and momentum ratios provided insights into hydrodynamics and sediment transport.

The model, designed using Froude similarity, replicates flow and sediment processes. The experiments revealed that momentum ratios strongly influence the size, location, and strength of secondary counter-rotating currents. These currents form due to flow deflection, reducing surface radial pressure via centrifugal forces. As a scour corridor develops, and secondary currents intensify, enhancing scour depth.

The experimental work highlighted the strong influence of tributary momentum ratios on the size, location, and strength of secondary counter-rotating currents. These currents initially form due to flow deflection, which lowers surface radial pressure through centrifugal forces, creating flow divergence—outward near the bottom and inward at the surface. As a scour corridor develops, secondary currents intensify, amplifying bed erosion and sediment transport. Flow recovery depends on discharge ratios, with near-equal flows stabilizing more quickly, while momentum asymmetry prolongs turbulence, leading to deeper scour holes, extended shear layers, and complex sediment deposition patterns. Downstream, velocities align longitudinally, and turbulence fades, gradually restoring flow stability.

These hydrodynamic processes shape sediment transport, influencing channel morphology and infrastructure stability. High-momentum tributaries create longer scour corridors, while secondary currents promote lateral bars and bank-attached deposits. Understanding these patterns enhances sediment management, informing strategies such as targeted dredging, structural reinforcements, and habitat restoration. Insights from this study can also guide flood defense design and port management, while experimental data offer a valuable benchmark for refining numerical models.

Author Contributions: J.N.F. proposed the theme and the setup and obtained the funding. L.A. conducted the experiments. J.N.F. drafted the first version of the paper. All authors contributed to the final writing and revision of this paper. All authors have read and agreed to the published version of the manuscript.

Funding: This research was funded by FEDER and Science and Technology Foundation under the scope of the Project MixFluv–Mixing Layers in fluvial systems (PTDC/ECI-EGC/31771/2017).

Institutional Review Board Statement: Not applicable.

Informed Consent Statement: Not applicable.

Data Availability Statement: The data that support the findings of this study are available from the corresponding author, J.N.F., upon reasonable request.

Acknowledgments: In addition to FEDER and FCT for funding this research, the authors would like to acknowledge Nuno Aido and César Costa for the valuable help during the experiments and Juana Fortes from the Harbours and Maritime Structures Division of LNEC for the support with the experimental facility.

Conflicts of Interest: The authors declare no conflicts of interest. The funders had no role in the design of this study; in the collection, analyses, or interpretation of data; in the writing of the manuscript, or in the decision to publish the results.

References

1. Mazgareanu, I.; Biron, P.M.; Buffin-Bélanger, T. A fuzzy GIS model to determine confluence morphological sensitivity to tributary inputs at the watershed scale. *Geomorphology* **2020**, *357*, 107095. [CrossRef]
2. Roy, A.G. Introduction to part I: River channel confluences. In *River Confluences, Tributaries and the Fluvial Networks*; Rice, S.P., Roy, A.G., Rhoads, B.L., Eds.; Willy: Chichester, UK, 2008; pp. 13–15. [CrossRef]
3. Mosley, M.P. An Experimental Study of Channel Confluences. *J. Geol.* **1976**, *84*, 535–562. [CrossRef]
4. Rhoads, B.L.; Sukhodolov, A.N. Field investigation of three-dimensional flow structure at stream confluences: 1. Thermal mixing and time-averaged velocities. *Water Resour. Res.* **2001**, *37*, 2393–2410. [CrossRef]
5. Best, J.L. Flow dynamics at river confluences: Implications for sediment transport and bed morphology. In *Recent Developments in Fluvial Sedimentology*; Etheridge, F.G., Flores, R.M., Harvey, M.D., Eds.; GeoScienceWorld: McLean, VA, USA, 1987; Volume 39, pp. 27–35.
6. Riley, J.D.; Rhoads, B.L. Flow structure and channel morphology at a natural confluent meander bend. *Geomorphology* **2012**, *163–164*, 84–98. [CrossRef]
7. Bradbrook, K.F.; Lane, S.N.; Richards, K.S. Numerical simulation of three-dimensional, time-averaged flow structure at river channel confluences. *Water Resour. Res.* **2000**, *36*, 2731–2746. [CrossRef]
8. Nazari-Sharabian, M.; Karakouzian, M.; Hayes, D. Flow Topology in the Confluence of an Open Channel with Lateral Drainage Pipe. *Hydrology* **2020**, *7*, 57. [CrossRef]
9. Canelas, O.B.; Ferreira, R.M.L.; Guillén-Ludeña, S.; Alegria, F.C.; Cardoso, A.H. Three-dimensional flow structure at fixed 70° open-channel confluence with bed discordance. *J. Hydraul. Res.* **2019**, *58*, 434–446. [CrossRef]
10. Covelli, C.; Cimorelli, L.; Pagliuca, D.N.; Molino, B.; Pianese, D. Assessment of Erosion in River Basins: A Distributed Model to Estimate the Sediment Production over Watersheds by a 3-Dimensional LS Factor in RUSLE Model. *Hydrology* **2020**, *7*, 13. [CrossRef]
11. Imhoff, K.S.; Wilcox, A.C. Coarse bedload routing and dispersion through tributary confluences. *Earth Surf. Dyn.* **2016**, *4*, 591–605. [CrossRef]
12. Guillén-Ludeña, S.; Franca, M.J.; Cardoso, A.H.; Schleiss, A.J. Hydro-morphodynamic evolution in a 90° movable bed discordant confluence with low discharge ratio. *Earth Surf. Process. Landf.* **2015**, *40*, 1927–1938. [CrossRef]
13. Guillén-Ludeña, S.; Franca, M.; Cardoso, A.; Schleiss, A. Evolution of the hydromorphodynamics of mountain river confluences for varying discharge ratios and junction angles. *Geomorphology* **2016**, *255*, 1–15. [CrossRef]
14. Leite Ribeiro, M.; Blanckaert, K.; Roy, A.G.; Schleiss, A.J. Flow and sediment dynamics in channel confluences. *J. Geophys. Res. Earth Surf.* **2012**, *117*, F01035. [CrossRef]
15. Yuan, S.; Tang, H.; Xiao, Y.; Qiu, X.; Zhang, H.; Yu, D. Turbulent flow structure at a 90-degree open channel confluence: Accounting for the distortion of the shear layer. *J. Hydro-Environ. Res.* **2016**, *12*, 130–147. [CrossRef]
16. Bombar, G.; Cardoso, A. Effect of the sediment discharge on the equilibrium bed morphology of movable bed open-channel confluences. *Geomorphology* **2020**, *367*, 107329. [CrossRef]
17. Lewis, Q.W.; Rhoads, B.L. LSPIV Measurements of Two-Dimensional Flow Structure in Streams Using Small Unmanned Aerial Systems: 2. Hydrodynamic Mapping at River Confluences. *Water Resour. Res.* **2018**, *54*, 7981–7999. [CrossRef]
18. Fernandes, J.N.; Leal, J.B.; Cardoso, A.H. Apparent friction coefficient in straight compound channels. *J. Hydraul. Res.* **2011**, *49*, 836–838. [CrossRef]
19. Zhang, T.; Feng, M.; Chen, K. Hydrodynamic characteristics and channel morphodynamics at a large asymmetrical confluence with a high sediment-load main channel. *Geomorphology* **2020**, *356*, 107066. [CrossRef]
20. Nazari-Giglou, A.; Jabbari-Sahebari, A.; Shakibaeinia, A.; Borghei, S.M. An experimental study of sediment transport in channel confluences. *Int. J. Sediment Res.* **2016**, *31*, 87–96. [CrossRef]
21. Alizadeh, L.; Fernandes, J. Turbulent Flow Structure in a Confluence: Influence of Tributaries Width and Discharge Ratios. *Water* **2021**, *13*, 465. [CrossRef]
22. Heller, V. Scale effects in physical hydraulic engineering models. *J. Hydraul. Res.* **2011**, *49*, 293–306. [CrossRef]
23. Goring, D.G.; Nikora, V.I. Despiking Acoustic Doppler Velocimeter Data. *J. Hydraul. Eng.* **2002**, *128*, 117–126. [CrossRef]
24. Fernandes, J.; Jónatas, R. Experimental flow characterization in a spiral vortex dropshaft. *Water Sci. Technol.* **2019**, *80*, 274–281. [CrossRef] [PubMed]
25. Wu, C. Towards linear-time incremental structure from motion, in 3DV 2013. In Proceedings of the 2013 International Conference on 3D Vision, Seattle, WA, USA, 29 June–1 July 2013; pp. 127–134. [CrossRef]
26. Boyer, C.; Roy, A.G.; Best, J.L. Dynamics of a river channel confluence with discordant beds: Flow turbulence, bed load sediment transport, and bed morphology. *J. Geophys. Res.* **2006**, *111*. [CrossRef]